Int. J. Adv. Eng. Pure Sci. 2023, 35(2): 193-202
DOI: 10.7240/jeps.1203686

RESEARCH ARTICLE / ARAŞTIRMA MAKALESİ

Energy and Exergy Analysis of an Innovative Power/Refrigeration Cycle: Kalina Cycle and Ejector Refrigeration Cycle

Candeniz SEÇKİN [1]

[1]*Marmara University, Engineering Faculty, Mechanical Engineering Department, Istanbul, Turkey*

Abstract
This study presents a thermodynamic analysis of a new combined power/refrigeration combined cycle. The combined cycle is comprised of two innovative cycles: Kalina cycle (KNC) and ejector refrigeration cycle (ERC) for power and refrigeration production, respectively. Recovery of heat process is involved in the design of the cycle to rise the energetic and exergetic efficiencies: emitted heat by the KNC is absorbed by the ERC in order to generate cooling. Effects of variation in KNC operational conditions which have direct effects on turbine power production capacity (temperature and pressure of the working fluid flow at the turbine inlet) on performance evaluation parameters of the system (energy efficiency, exergy efficiency, energetic and exergetic content of produced refrigeration and net power) are investigated. A detailed discussion of the results is also reported. Energetic and exergetic efficiency results are substantially dominated by generated power, i.e., KNC parameters which impose direct effect on turbine power production performance is of superior importance to rise the energy and exergy efficiencies.
Keywords: Ejector refrigeration, Kalina cycle, Combined cycle, Energy efficiency, Exergy efficiency

Öz
Bu çalışmada yeni bir bileşik güç/soğutma çevriminin termodinamik analizi sunulmuştur. Bileşik çevrim iki yeni çevrimin birleşiminden oluşmuştur: güç Kalina çevriminde (KNC), soğutma ise ejektörlü soğutma çevriminde (ERC) üretilmektedir. Sistem enerji ve ekserji verimlerini yükseltmek için bileşik çevrim tasarımında ısı geri kazanımı prosesine yer verilmiştir: KNC tarafından salınan ısı ERC tarafından alınmakta ve soğutma üretiminde kullanılmaktadır. KNC çalışma parametrelerinden türbin güç üretim kapasitesine direkt etkisi olan parametrelerin değişiminin (çevrim akışkanının türbin girişindeki sıcaklık ve basıncı), bileşik çevrim enerji ve ekserji verimi ve ayrıca, üretilen güç ve soğutmanın enerji ve ekserji karşılıklarına olan etkileri incelenmiştir. Elde edilen sonuçların detaylı incelemesi de çalışmada sunulmuştur. Enerji ve ekserji veriminin baskın şekilde bileşik çevrimde üretilen güç tarafından belirlendiği tespit edilmiştir. Diğer bir deyişle, bileşik çevrimin enerji ve ekserji verimini yükseltmek için KNC çevriminde güç üretim kapasitesini direkt etkileyen faktörler öncelikli olarak incelenmelidir.
Anahtar Kelimeler: Ejektörlü soğtuma, Kalina çevrimi, Bileşik çevrim, Enerji verimi, Ekserji verimi

I. INTRODUCTION

Increasing rate of growth in energy demand of the World is a natural consequence of rising World population. It is reported that total energy requirement of the World in 2035 is predicted to be almost 35% higher than that of 2010 [1]. The increasing demand for energy brings noticeable amount of fossil based fuel consumption together with accompanying unfavorable effects of fossil fuel burning on the environment such as greenhouse gas emissions. Gas emissions resulting from combustion processes in the course of electricity and heat production constitute almost 60% of total greenhouse emissions [2] which apparently points out the necessity of taking actions against environmental damage caused by fossil fuel use in energy generation. In this regard, utilization of energy resources in more efficient ways poses paramount importance to resuce fossil fuel consumption and its harmful environmental effects. Among many different methods which have been developed and employed for this purpose, use of waste heat recovery technologies in energy generation and industrial processes have been a topic of recent interest and one of the significant areas of research [2-6]. In this context, the combined cycle of cooling and power (cogeneration cycle) can be regarded as a promising future trend which enables to use the "otherwise" wasted heat of one thermodynamic cycle, in the other cycle to produce additional system outputs, simultaneously [7-9]. This heat recovery process within the system provides the advantage of lower fuel consumption than that of required in separate

Corresponding Author: Candeniz SECKIN, **Tel:** 0212 777 37 31, **e-posta:** candeniz.seckin@marmara.edu.tr
Submitted: 13.11.2022, **Revised:** 21.01.2023, **Accepted:** 26.03.2023

generation of the same outputs by conventional thermodynamic cycles. Energy efficiency increase in cogeneration plants relative to production of power and refrigeration in single plants is measured between 10-30% in several studies [7, 10-11].

In the past decades, use of binary mixtures in power generating cycles receives considerable attention. Due to the inconstant temperature characteristics of binary mixtures during constant pressure phase change processes (condensation, evaporation, etc.), better temperature matching is rendered by binary mixtures between the refrigerant and thermal reservour relative to pure working fluids. As a result, reduction of irreversibility generation (exergy destruction) is observed in the total cycle [12-15]. KNC is presented by Dr. Alexander Kalina as a heat driven, binary mixture (ammonia–water) using power generation cycle [16-17]. By virtue of above mentioned profits of using binary mixtures in power cycles, relative to traditional power cycles [18-20] and other cycles [21-26], higher performance of KNC is reported in the literature.

Ejector refrigeration cycle (ERC) receives considerable attention from scientists, researchers, and engineers due to its high potential of effective low grade heat recovery which provides a cost-effective process, lower environmental damage and reduced energy consumption in refrigeration generation [27-29]. Additionally, ejector itself offers low cost of operation, installation and maintenance, simple operational mechanism with board range of refrigerant operation ability [30-33]. All these remarkable properties of ejector refrigeration systems render ejector refrigeration suitable to utilize the waste heat in refrigeration production which forms the main idea of this present study, i.e., ERC receives the waste heat rejected by the KNC in the analyzed combined cycle in this study. ERC operational principals are reported in detail in further sections. Analyses of ERC use in power/refrigeration combined cycles have been also reported in several studies so far [34-41].

Parametric analysis of a combined cycle which consist of unconventional power and refrigeration cycles (KNC and ERC) is carried out and a detailed discussion of the obtained results is reported in this study. Power is produced in the KNC and heat which is released from the KNC is regained by transferring it to the ERC in order to generate refrigeration. ERC is preferred to be occupied in the cycle since ERC has the capability of producing cooling effect with high efficiency by using low temperature sources [42-44]. Hence, ERC is quite suitable to regain the low-temperature waste heat of KNC in this present study. To the best of the authors' knowledge, design of the proposed coupled KNC and ERC cycle in this present study has not been presented so far in the existing literature, hence, the proposed combination cycle is novel. Modeling and simulation of the system are conducted by EES software which is extensively reported below. The results of the study indicate the effects of system operational conditions (temperature and pressure of the working fluid flow at the turbine inlet) on system output parameters (system energy efficiency, exergy efficiency, energetic and exergetic content of refrigeration and net power). Discussion of the results and behind physical mechanisms are also extensively presented in this study.

II. SYSTEM OPERATIONAL MECHANISM

Combined cycle schematic view is provided in Figure 1. The combined cycle produces two outputs: "power" is generated by the turbine in the KNC and "cooling" is supplied by the evaporator in ERC. As shown in Figure 1, heat which is discharged by the condenser of the KNC is transferred to the ERC by a heat exchanger and is used to drive the operation of the ERC cycle.

The working fluid of the KNC (ammonia-water mixture, NH3-H2O) exhibits a varying temperature profile during evaporation and condensation processes depending on the composition of the mixture. This non-isothermal profile of working fluid in KNC provides a closer temperature profile between the thermal source and the working fluid compared to isothermal temperature profile of pure substances in evaporation and condensation processes. The improved thermal match results in more efficient heat exchange and less irreversibility production during heat-transfer process which yields raised energy and exergy efficiencies [13, 45-46]. Heat is dispatched to the KNC working fluid in a heat exchanger (HE I in Figure 1). Two phase working fluid leaves HE I and is transferred to the separator. Vapor part of the working fluid (ammonia rich vapor) is separated from liquid part (water rich liquid) in the separator and ammonia rich vapor is dispatched to the turbine where the power generation takes place. On the other side, water rich liquid passes through a heat exchanger (High Temperature Regenerator - HTR) and is expanded to a lower pressure. After leaving the turbine, ammonia rich vapor merges with water rich liquid to reform the working fluid of KNC. The working fluid first enters into the low temperature recuperator (LTR) and then the heat exchanger (HE II in Figure 1) which acts as the condenser of the KNC and also heat supplier of the ERC cycle, i.e., above mentioned heat transfer process between the ERC and KNC takes place in HE II. The LTR and HTR are used to perform additional heat recovery in KNC by interchanging the energy of KRC working fluid. At the HE II exit, binary mixture is at saturated state and its pressure is increased by pump I. Afterwards isobaric heat transfer processes to the KRC working fluid occur in LTR and HTR to rise the working fluid temperature. Finally, the ammonia-water solution reaches the HE I to complete the cycle [15, 29, 31].

Schematic representation of ejector refrigeration cycle (ERC) and its main components are seen in Figure 2.

Rejected heat of KNC is absorbed by working fluid of ERC (R134a) which is also the driving heat of refrigeration cycle. Refrigerant (ERC working fluid) is evaporated in HE II and is delivered to the ejector in vapor phase which poses "first flow" of the ejector. The other vapor flow comes from the evaporator (called "secondary flow") and is transferred to the ejector (as seen in Figure 3). First flow gets into a convergent – divergent nozzle which is namely the "primary nozzle". At the throat of the primary nozzle ("t" in Figure 3), first flow is chocked and supersonically expands and reaches the primary nozzle outlet at low pressure which creates a vacuum effect on secondary flow. As a result, the secondary flow gets into the secondary nozzle of the ejector as seen in Figure 3. At the end of the nozzles, both of the flows are supersonic as a result of pressure decline in the nozzles. The flows enter into the "mixing zone" (Figure 3) in which mixing of two streams finishes up at "a" in Figure 3. Then, compression of the mixed flow is seen due to the occurrence of a shock wave ("b" in Figure 3) and thereby, increase in refrigerant pressure is accompanied by a rapid drop in velocity. Pressure at the condenser and the diffuser exit are identical. [27,29,31,47-49]. As seen in Figure 2, after the ejector, condensation of the refrigerant is performed in the condenser and heat is released out of the ERC. At the condenser outlet, liquid refrigerant is separated into two refrigerant streams: one stream is dispatched to the pump II to increase its pressure before passing through the HE II. The other stream expands through a valve to equalize its pressure to evaporator pressure. Refrigeration is supplied by the isobaric evaporation of the refrigerant (absorbing heat from the cooled space to the refrigerant) in the evaporator [27, 47-49].

III. THERMODYNAMIC MODELLING AND COMPUTATIONAL PROGRAMING

Below listed assumptions are applied in the modeling of the combined cycle [29-31,39,49-51]:
• Steady-state operating conditions exist.
• Fluid flows are one dimensional, frictionless and uniform through the cross-section.
• Pressure losses and the leakage of working fluids in system components are disregarded.
• Except the condensers and evaporator, no heat transfer between the system and the surrounding.
• Energy losses in the turbine, ejector and pumps are computed by means of isentropic efficiencies.
• Kinetic energy and potential energy changes of the fluid across the system components are neglected.

Applied assumption in KNC modeling is the following [29,31,39]:
• Saturated flow conditions at points 2, 3 and 9 in Figure 1.

Applied assumptions in ERC modelling are presented in the followings [29,31,47,52]:
• Stagnation velocity of the refrigerant at the inlet and outlet of the ejector.
• Saturated condition at the exit of condenser II, evaporator and heat exchanger exit between KRC and ERC.
• Entrainment ratio is constant.
• The secondary flow reaches supersonic conditions at the nozzle exit.

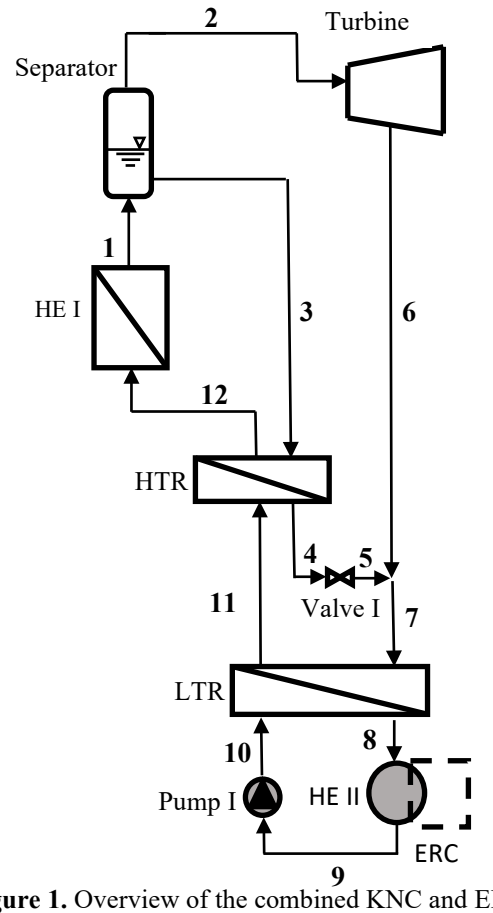

Figure 1. Overview of the combined KNC and ERC cycle.

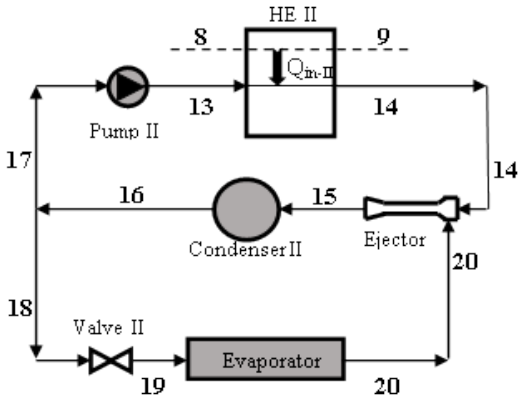

Figure 2. Schematic representation of ERC.

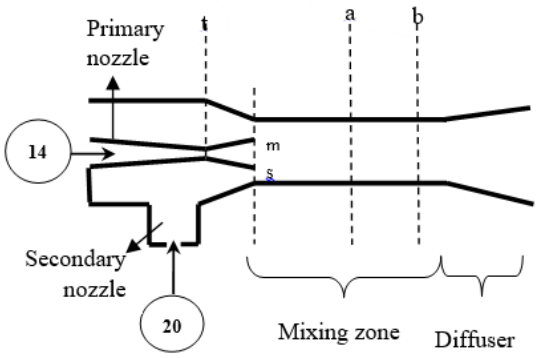

Figure 3. Ejector design.

Simulation program of the combined cycle is built in Engineer Equation Solver (EES) software. EES databank provides the physical properties of KNC working fluid (NH3-H2O, ammonia-water mixture) and ERC refrigerant (R134a).

Mathematical formulas which are used in the modelling of the KNC and ERC are presented below. In the formulas, mass flow rate, concentration, pressure, temperature, quality, enthalpy and entropy of working fluid are ṁ, x, P, T, q, h, s, respectively. Subscripted state-points of the system are seen in Figures 1–3. Conservation of mass, momentum and energy equations used in the thermodynamic model of the combined cycle are seen in Equations (1-40).

3.1. Kalina Cycle

In Equation (1), mathematical formula for the ammonia concentration in total binary mixture (x) is reported. Briefly "concentration" refers to ammonia concentration in further parts of this study.

$$x = \frac{\dot{m}_{NH3}}{\dot{m}_1} \quad \textbf{(1)}$$

where $\dot{m}_{NH3}$ is the ammonia mass flow rate and $\dot{m}_1$ is the KNC working fluid total mass flow rate.

Conservation of mass equations applied to the separator of the KNC are presented as the following.

$$\dot{m}_1 = \dot{m}_2 + \dot{m}_3 \quad \textbf{(2)}$$

$$\dot{m}_1 x_1 = \dot{m}_2 x_2 + \dot{m}_3 x_3 \quad \textbf{(3)}$$

Turbine isentropic efficiency (η_{tur}) is shown in below equation to determine the enthalpy change across the turbine (h_2-h_6) where subscript "is" stands for isentropic and $\dot{W}_{tur,is}$ is power generation by an isentropic process in the turbine.

$$\eta_{tur} = \frac{\dot{W}_{tur}}{\dot{W}_{tur,is}} = \frac{h_2 - h_6}{h_2 - h_{6,is}} \quad \textbf{(4)}$$

$\dot{W}_{tur}$ is the KNC power production which is obtained by the following:

$$\dot{W}_{tur} = \dot{m}_2 \, (h_2 - h_6) \quad \textbf{(5)}$$

Below equation is applied for the mixing process of the water rich and ammonia rich solution flows at the turbine exit:

$$\dot{m}_7 h_7 = \dot{m}_6 h_6 + \dot{m}_5 h_5 \quad \textbf{(6)}$$

For the isenthalpic expansion in valve I, below relation is applied.

$$h_4 = h_5 \quad \textbf{(7)}$$

For the heat transfer processes in LTR and HTR, below equations are applied where TTD is terminal temperature difference of LTR.

$$T_{11} = T_7 - TTD \quad \textbf{(8)}$$

$$\dot{m}_3 (h_3 - h_4) = \dot{m}_{11} (h_{12} - h_{11}) \quad \textbf{(9)}$$

Isentropic efficiency of the pump ($\eta_{p\text{-}I}$) is used in Equation (10) to determine the enthalpy change across the pump (h_{10}-h_9) where subscript "is" stands for isentropic and $\dot{W}_{p\text{-}I,is}$ is power consumption in an isentropic process of the pump.

$$\eta_{p\text{-}I} = \frac{\dot{W}_{p\text{-}I,is}}{\dot{W}_{p\text{-}I}} = \frac{h_{10,is} - h_9}{h_{10} - h_9} \quad \textbf{(10)}$$

Following equation is used to determine the power requirement of pump I ($\dot{W}_{p\text{-}I}$):

$$\dot{W}_{p\text{-}I} = \dot{m}_9 \, (h_{10} - h_9) \quad \textbf{(11)}$$

To determine the rate of heat transfer between KNC and ERC ($\dot{Q}_{cond\text{-}I}$), Equation (12) and Equation (13) are applied to the LTR and conderser I, respectively.

$$\dot{m}_{11} (h_{11} - h_{10}) = \dot{m}_7 (h_7 - h_8) \quad \textbf{(12)}$$

$$\dot{Q}_{cond\text{-}I} = \dot{m}_8 \, (h_8 - h_9) \quad \textbf{(13)}$$

3.2. ERC Analysis

Entrainment ratio (w) equation is seen below where $\dot{m}_{14}$ and $\dot{m}_{20}$ are mass flow rates of the first flow and the secondary flow.

$$w = \frac{\dot{m}_{20}}{\dot{m}_{14}} \quad \textbf{(14)}$$

Below presented formulas are derived to model the ejector and total refrigeration cycle where $\dot{m}_{ERC}$ is the ERC refrigerant mass flow rate, $P_{c\text{-}ERC}$, P_{epr}, $P_{HE\text{-}II}$ are pressure of condenser II, evaporator and heat exchanger II, respectively. Additionally, η_m, η_s, η_d, $\eta_{p\text{-}II}$ are isentropic efficiency of primary nozzle, secondary nozzle, diffuser and pump II, respectively.

Owing to the chocking of the first flow at the throat of the primary nozzle ("t" in Figure 3), characteristics of the flow converts into subsonic to supersonic. As a result, Mach number is unity and velocity (V_t) is equal to sound speed (C_t) at the throat. C_t is computed by Equation (15) and is used in Equations (16-17) to determine the cross-sectional area of the throat (A_t). v_t is the specific volume of the refrigerant at the throat of the primary nozzle.

$$C_t = f(P_t, h_t) \quad \textbf{(15)}$$

$$V_t = \sqrt{2\,(h_{14} - h_t)} \quad \textbf{(16)}$$

$$\dot{m}_{14} = \dot{m}_t = \left(\frac{1}{1+w}\right) \dot{m}_{ERC} = \frac{V_t\, A_t}{v_t} \quad \textbf{(17)}$$

Primary nozzle isentropic efficiency (η_m) is used to determine the specific enthalpy at primary nozzle exit (h_m) as seen in Equation (18) ($h_{m,is}$ is the first flow enthalpy at primary nozzle exit after an isentropic process).

$$\eta_m = \frac{h_{14} - h_m}{h_{14} - h_{m,is}} \quad \textbf{(18)}$$

Velocity (V_m) and area (A_m) of the primary nozzle are obtained by the following equations where v_m is the refrigerant specific volume at the primary nozzle outlet.

$$V_m = \sqrt{2\,(h_{14} - h_m)} \quad \textbf{(19)}$$

$$\dot{m}_{14} = \dot{m}_m = \left(\frac{1}{1+w}\right) \dot{m}_{ERC} = \frac{V_m\, A_m}{v_m} \quad \textbf{(20)}$$

Above given procedure is applied to determine the refrigerant properties at the secondary nozzle. Mach number is unity in cross section s in Figure 3. Following equations are used to determine the cross-sectional area at the secondary nozzle exit (A_s) where v_s is the specific volume of the refrigerant and $h_{s,is}$ is isentropic enthalpy of secondary flow at cross section s in Figure 3.

$$\eta_s = \frac{h_{20} - h_s}{h_{20} - h_{s,is}} \quad \textbf{(21)}$$

$$V_s = \sqrt{2\,(h_{20} - h_s)} \quad \textbf{(22)}$$

$$\dot{m}_{20} = \dot{m}_s = \left(\frac{w}{1+w}\right) \dot{m}_{ERC} = \frac{V_s\, A_s}{v_s} \quad \textbf{(23)}$$

When saturated mixture phase refrigerant is seen at the cross sections of t, m and s in Figure 3, critical flow properties of the refrigerant is obtained by Henry and Fauske method which is broadly explained in [28,53-55].

Velocity and enthalpy of the mixed refrigerant at cross section "a" are computed by the following equations where ϕ, V_a, A_a and v_a are coefficient of frictional loss, velocity, cross-sectional area and specific volume at "a" in the ejector (Figure 3), respectively.

$$A_a = A_m + A_s \quad \textbf{(24)}$$

Conservation of mass equation:

$$\dot{m}_a = \dot{m}_m + \dot{m}_s = \dot{m}_{ERC} \quad \textbf{(25)}$$

Conservation of momentum equation:

$$\begin{aligned} &P_a\, A_a + \dot{m}_{ERC}\, V_a = \\ &\phi\left(P_m\, A_m + \dot{m}_m\, V_m + P_s\, A_s + \dot{m}_s\, V_s\right) = \\ &P_a\, A_a + \frac{A_a\, V_a^2}{v_a} = \\ &\phi\left(P_m\, A_m + \frac{A_m\, V_m^2}{v_m} + P_s\, A_s + \frac{A_s\, V_s^2}{v_s}\right) \end{aligned} \quad \textbf{(26)}$$

Conservation of energy equation:

$$\dot{m}_{ERC}\left[h_a + \frac{V_a^2}{2}\right] = \dot{m}_m\left[h_m + \frac{V_m^2}{2}\right] + \dot{m}_s\left[h_s + \frac{V_s^2}{2}\right] \quad \textbf{(27)}$$

Shock occurs at "b" in Figure 3 and after the shock, the flow characteristics transfers into subsonic from supersonic flow. Rankine-Hugoniot equations are utilized to obtain the properties of the fluid after the shock occurs [43, 56]. Related equations are given below in which subscript "b" signifies "after-shock" thermodynamic properties of the refrigerant.

$$\frac{P_b}{P_a} = \frac{2\,k\,M_a^2 - (k-1)}{k+1} \quad \textbf{(28)}$$

$$\frac{\rho_b}{\rho_a} = \frac{v_a}{v_b} = \frac{(k+1)\,M_a^2}{(k-1)\,M_a^2 + 2} \quad \textbf{(29)}$$

In Equations (28-29), Ma and k are Mach number and specific heat ratio (c_p/c_v) at "a" in Figure 3, respectively. Densities at "a" and "b" are ρ_a and ρ_b, respectively.

Specific enthalpy of the refrigerant at the exit of the diffuser part of the ejector (h_{15}) is determined by Equations (30-31). Equation (30) is obtained from conservation of energy principle and Equation (31) is

based on isentropic efficiency of the diffuser where $h_{15,is}$ is isentropic enthalpy of the refrigerant at the diffuser exit.

$$\dot{m}_{ERC}\, h_{15} = \dot{m}_{14}\, h_{14} + \dot{m}_{20}\, h_{20} \quad (30)$$

$$\eta_d = \frac{h_{15,is} - h_b}{h_{15} - h_b} \quad (31)$$

Energy interaction between the KNC and ERC takes place in HE II (Figure 2) which also acts as the condenser of the KNC (condenser I). Rate of heat transfer from KNC to ERC ($\dot{Q}_{in,II}$) is computed by means of Equation (32) as presented below. Additionally, rate of heat rejection by ERC to the surrounding ($\dot{Q}_{cond,II}$) and rate of heat absorbed from cooled space by the ERC (cooling capacity) ($\dot{Q}_{ref}$) are obtained by the following equations.

$$\dot{Q}_{in\text{-}II} = \dot{m}_{13}\,(h_{14} - h_{13}) \quad (32)$$

$$\dot{Q}_{cond\text{-}II} = \dot{m}_{ERC}\,(h_{15} - h_{16}) \quad (33)$$

$$\dot{Q}_{ref} = \dot{m}_{19}\,(h_{20} - h_{19}) \quad (34)$$

Rate of power consumption by pump II in ERC ($\dot{W}_{p\text{-}II}$) is determined by below equations.

$$\dot{W}_{p-II} = \frac{v_{17}\,(P_{13} - P_{17})}{\eta_{p-II}}\,\dot{m}_{13} \quad (35)$$

$$\dot{W}_{p-II} = \dot{m}_{13}\,(h_{13} - h_{17}) \quad (36)$$

3.3. System Output Parameters

Mathematical formulas to compute the net power production ($\dot{W}_{net}$) and energy efficiency (η_{cc}) of the combined cycle are seen in Equations (37-38), respectively.

$$\dot{W}_{net} = \dot{W}_{tur} - \dot{W}_{p-I} - \dot{W}_{p-II} \quad (37)$$

$$\eta_{cc} = \frac{\dot{W}_{net} + \dot{Q}_{ref}}{\dot{Q}_{in\text{-}I}} \quad (38)$$

Regarding the mathematical expressions for system exergetic output parameters, exergy efficiency of the combined cycle (η_{ex}) is presented in Equation (39) where $\dot{E}x_{in\text{-}I}$ is the rate of exergy content of the energy provided to the combined cycle in HE I, $\dot{E}x_{Qref}$ is the rate of exergetic equivalent of the refrigeration capacity and $\dot{E}x_{Wnet}$ is the exergetic equivalent of the net power produced by the combined cycle. $\dot{E}x_{Qref}$ and $\dot{E}x_{in\text{-}I}$ are obtained by Equations (40-41) [29,31,57-59].

$$\eta_{ex} = \frac{\dot{E}x_{Wnet} + \dot{E}x_{Qref}}{\dot{E}x_{in\text{-}I}} = \frac{\dot{W}_{net} + \dot{E}x_{Qref}}{\dot{E}x_{in\text{-}I}} \quad (39)$$

$$\dot{E}x_{Qref} = \dot{m}_{19}\,\left[(h_{19} - h_{20}) - T_0\,(s_{19} - s_{20})\right] \quad (40)$$

$$\dot{E}x_{in\text{-}I} = \dot{m}_{1}\,\left[(h_{12} - h_1) - T_0\,(s_{12} - s_1)\right] \quad (41)$$

IV. RESULTS AND DISCUSSION

The results of the analysis indicate the effects of variation in considered operational parameters of KNC (turbine inlet temperature (T_2) and pressure (P_2)) to the selected system parameters of the combined cycle which are: energetic efficiency (η_{cc}), exergetic efficiency (η_{ex}), power generation ($\dot{W}_{net}$), rate of refrigeration ($\dot{Q}_{ref}$), exergy of produced power ($\dot{E}x_{Wnet}$) and rate of refrigeration exergy ($\dot{E}x_{Qref}$). T_2 and P_2 are chosen to be investigated in this study since these are the main operational parameters of KNC which directly effects the power production performance of the turbine. Operational conditions remain constant in the performed numerical analysis as presented in Table 1.

Table 1. Operational parameters (subscripted state-points are seen in Figures 1–3).

Parameter (unit)	
$\dot{Q}_{in\text{-}I}$ (kW)	1000
T_3 (°C)	120
P_3 (kPa)	3500
T_9 (°C)	15
x_1 (%)	70
$\dot{m}_1$ (kg/s)	0.98
$\dot{m}_{ERC}$ (kg/s)	0.85
$\eta_{p\text{-}I}/\eta_{p\text{-}II}/\eta_{tur}/\eta_m/\eta_s/\eta_d$ (%)	80/80/80/90/90/90
$P_{c\text{-}ERC}$ (kPa)	850
P_{epr} (kPa)	415
$P_{HE\text{-}II}$ (kPa)	2635.3

In Figure 4, variation of $\dot{W}_{net}$, $\dot{Q}_{ref}$ and η_{cc} at different turbine inlet pressures (P_2) is presented. Work production potential of the KNC is directly influenced by P_2 and thereby, η_{cc} results are also affected by P_2 based on Equation (38). On the other side, turbine inlet pressures (P_2) is identical to HE I pressure and based on Equation (41), pressure of HE I quantifies the supplied exergy to the combined cycle ($\dot{E}x_{in\text{-}I}$). Thus, P_2 also imposes a direct influence on η_{ex} results of the combined cycle based on Equation (39). Hence, among all the operational parameters, turbine inlet pressure (P_2) is expected to be one of the most prevailing parameters on the η_{cc} and η_{ex} efficiencies of the combined cycle. As seen in Figure 4, thermal efficiency (η_{cc}) rises but the rate of rise lowers as P_2 rises. It must be stated here that, among the three constituents of $\dot{W}_{net}$ results (Equation (37)), $\dot{W}_{tur}$ constitutes the greatest part, i.e., the effect of power consumption by the pumps ($\dot{W}_{p\text{-}I}$ and $\dot{W}_{p\text{-}II}$) on $\dot{W}_{net}$ are inconsiderable compared to that of $\dot{W}_{tur}$. In other words, magnitude of $\dot{W}_{net}$ is almost entirely characterized by $\dot{W}_{tur}$. As presented in Equation (5), turbine power production is directly proportional to the rate of KNC working fluid mass flow which is dispatched to the turbine ($\dot{m}_2$) and enthalpy difference (h_2-h_6). It is seen that as P_2 heightens, enthalpy difference and mass flow rate display reverse patterns: (h_2-h_6) grows while $\dot{m}_2$ ascends. As a result, $\dot{W}_{tur}$ gets

higher owing to the growing (h_2-h_6) but the rate of increase declines with decreasing $\dot{m}_2$ as P_2 rises (Figure 4). Since the operational parameters of ERC remains constant during the analysis, physical conditions and mass flow rate of the refrigerant are constant at the inlet and outlet of the evaporator, i.e., refrigeration generation by ERC ($\dot{Q}_{ref}$) is kept constant based on Equation (34) ($\dot{Q}_{ref}$ is 44.65 kW). Hence, based on Equation (38), thermal efficiency (η_{cc}) of the combined cycle is predominantly affected by variation of $\dot{W}_{net}$ and similar trends of the η_{cc} and $\dot{W}_{net}$ curves are clearly seen in Figure 4.

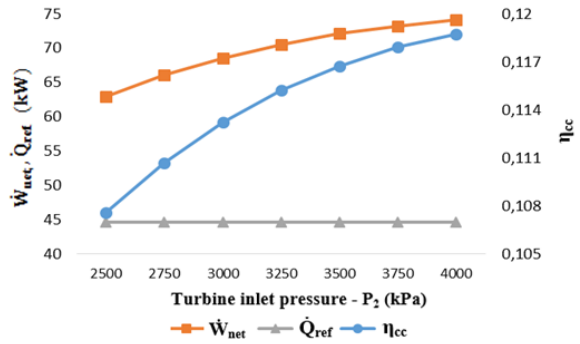

Figure 4. $\dot{W}_{net}$, $\dot{Q}_{ref}$ and η_{cc} versus P_2.

Figure 5 presents the effect of increasing turbine inlet pressure (P_2) on $E\dot{x}_{Wnet}$, $E\dot{x}_{Qref}$ and η_{ex} results of the considered combined cycle. Figure 5 indicates that exergy efficiency (η_{ex}) rises with growing P_2. As mentioned above, in spite of the variation of P_2, working parameters and physical properties of refrigerant remain constant in ERC. This brings constant $E\dot{x}_{ref}$ based on Equation (40) ($E\dot{x}_{Qref}$ is 12.22 kW). By definition, exergy of produced power ($E\dot{x}_{Wnet}$) is directly equal to $\dot{W}_{net}$ while the rate of refrigeration exergy ($E\dot{x}_{Qref}$) is substantially less than $\dot{Q}_{ref}$. Thereby, $E\dot{x}_{ref}$ is considerably lower than $E\dot{x}_{Wnet}$ and hence, based on Equation (39), exergy efficiency (η_{ex}) results are prevailingly shaped by $E\dot{x}_{Wnet}$. As a result, η_{ex} and $E\dot{x}_{Wnet}$ curves exhibit a similar trend in Figure 5: both of them increases with increasing P_2. Additionally, increasing results of η_{ex} is also supported by reducing $E\dot{x}_{in\text{-}I}$. (see Equation (39)) but its influence on η_{ex} is quite marginal owing to the slight drop of $E\dot{x}_{in\text{-}I}$ as P_2 rises.

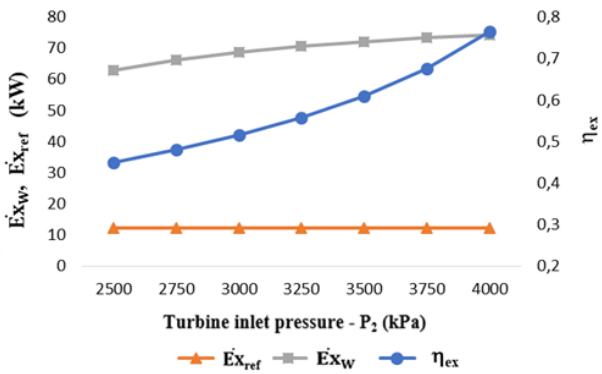

Figure 5. $E\dot{x}_{Wnet}$, $E\dot{x}_{Qef}$ and η_{ex} versus P_2.

Figure 6 shows the $\dot{W}_{net}$, $\dot{Q}_{ref}$ and η_{cc} results versus the temperature at the turbine inlet (T_2). Temperature of the KNC working fluid at the turbine inlet (T_2) has nonignorable impact on η_{cc} and η_{ex} results based on the similar reasons to those for P_2: increasing T_2 affects $\dot{W}_{tur}$ and hence $\dot{W}_{net}$ in Equation (38) and $E\dot{x}_{WnetI}$ in Equation (39). The results of the performed analysis point out that $\dot{m}_2$ and (h_2-h_6) are ascending with increasing T_2 which directly yields rising $\dot{W}_{tur}$ (it can be regarded as identical to $\dot{W}_{net}$ with negligible error as stated above). Hence, rising $\dot{W}_{net}$ yields increasing η_{cc} based on Equation (38). Therefore, direction of curves which represent the variation of $\dot{W}_{net}$ and η_{cc} is upward with increasing T_2 in Figure 6. Since variation of T_2 has no influence on ERC operational conditions (which are constant as presented in Table 1), refrigerant properties and hence $\dot{Q}_{ref}$ production of ERC is constant in Figure 6 ($\dot{Q}_{ref}$ is 44.65 kW). Strong correlation between $\dot{W}_{net}$ and η_{cc} (Figure 6) is also supported by constant $\dot{Q}_{ref}$ based on Equation (38).

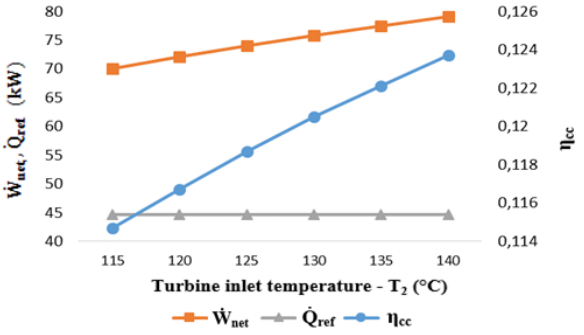

Figure 6. $\dot{W}_{net}$, $\dot{Q}_{ref}$ and η_{cc} versus T_2.

Figure 7 depicts the effect of increasing turbine inlet temperature (T_2) on $E\dot{x}_{Wnet}$, $E\dot{x}_{Qref}$ and η_{ex} results of the considered combined cycle. It is seen that, exergetic efficiency (η_{ex}) graph indicate a reverse characteristics to that of η_{cc}. η_{ex} results decrease but the rate of decrease gets lower as T_2 rises. Because magnitude of $\dot{W}_{net}$ is directly equal to that of $E\dot{x}_{Wnet}$, rising $E\dot{x}_{Wnet}$ is seen in Figure 7 due to the above stated reasons for the rise of $\dot{W}_{net}$. On the other hand, it is determined that $E\dot{x}_{in\text{-}I}$ (rate of exergy supply to the combined cycle in HE I) is increasing with growing T_2 and the rate of

increase is greater than that of $E\dot{x}_{Wnet}$. As a result, based on Equation (39), $E\dot{x}_{in\text{-}I}$ prevails η_{ex} of the combined cycle more than $E\dot{x}_{Wnet}$ and η_{ex} gets lower in the analysed range of T_2.

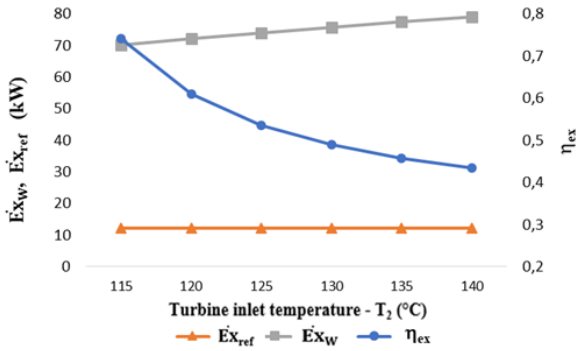

Figure 7. $E\dot{x}_{Wnet}$, $E\dot{x}_{Qef}$ and η_{ex} versus T_2.

V. CONCLUSION

In this current study, thermodynamic analysis of a combined cycle which consist of two innovative thermodynamic cycles for power and refrigeration generation (KNC and ERC) is presented. Heat recovery process with the proposed design Presented design of the heat recovery processes within the combined cycle is novel and has never been analyzed in the available literature. Combined cycle is designed in such a manner so that rejected heat by the KNC is transferred to the ejector refrigeration cycle. Proposed way of combination in the design of the The system is analyzed from energetic and exergetic aspects, obtained results are discussed to provide deeper understanding to the system's physical mechanism and to bring some light to the effect of operational conditions on energetic and exergetic performance of the considered combined cycle. The results indicate the effects of considered KNC operational parameters (P_2 and T_2) on output parameters of the system: rate of refrigeration generation ($\dot{Q}_{ref}$), rate of net power output ($\dot{W}_{net}$), energy and exergy efficiency (η_{cc}, η_{ex}) and exergy of produced power and refrigeration ($E\dot{x}_{Wnet}$, $E\dot{x}_{Qref}$). The main findings of this research are outlined by the followings:

- As P_2 grows in the range from 2500 kPa to 4000 kPa, η_{cc} and η_{ex} curves exhibit a similar trend: η_{cc} and η_{ex} results are rising with increasing P_2. In the considered interval of P_2, η_{cc} and η_{ex} of the combined cycle increases by 10% and 70%, respectively. It is determined that P_2 directly effects the work production capacity of the turbine and hence, total energy and exergy produced by the combined cycle gets higher. As a result, increase of η_{cc} and η_{ex} is observed with rising P_2.
- Rise of T_2 in the range of 115–140°C shows reverse pattern for η_{cc} and η_{ex}: η_{cc} heightens by 7% while η_{ex} drops by 41% in the analyzed range of T_2. It is obtained that increasing T_2 results in ascending results of $\dot{W}_{net}$ and $E\dot{x}_{in\text{-}I}$ which lead the above mentioned reverse trends in η_{cc} and η_{ex} of the combined cycle.
- The results indicate that η_{cc} and η_{ex} of the combined cycle are highly prevailed by net power production ($\dot{W}_{net}$) which is almost identical to turbine power production in the KNC. Hence, operational parameters which effects the power production performance of the turbine must be primarily analyzed to operate the cycle with high energy or exergy efficiencies.

REFERENCES

[1] Internal Energy Agency. "World Energy Outlook. Paris: Internal Energy Agency; 2012. [cited 2022 October 5]." (2012).

[2] B. Herzog, P. Jonathan, K.A. Baumert. "Navigating the numbers- greenhouse gas data and international climate policy. Washington: World Resources Institute: [cited 2022 October 5]." (2005).

[3] N. Ozalp. Utilization of heat, power, and recovered waste heat for industrial processes in the U.S. chemical industry. ***J Energy Resour.,*** 131, 022401-1- 022401-11, (2009).

[4] A. Khaliq, R. Kumar, I. Dincer. Exergy analysis of an industrial waste heat recovery based cogeneration cycle for combined production of power and refrigeration. ***J Energ Resour.,*** 131, 022402-1- 022402-9, (2009).

[5] K. Sarmah, P. Gupta. Refrigeration by waste heat recovery. ***International Journal of Interdisciplinary Research,*** 3, 1-7, (2017).

[6] D. Brough, H. Jouhara. The aluminum industry: a review on state-of-the-art technologies, environmental impacts and possibilities for waste heat recovery. ***International Journal of Thermofluids***, 1-2, 1-39. (2020).

[7] A.O. Arnas, D.D. Boettner, S.A. Norberg, G. Tamm, J.R. Whipple .On the teaching of performance evaluation and assessment of a combined cycle cogeneration system. ***J Energ Resour***, 131, 025501-1- 025501-7, (2011).

[8] U. Cakir, K. Comakli, F. Yuksel. The role of cogeneration systems in sustainability of energy. ***Energy Convers Manage.***, 63, 196–202, (2012).

[9] M.D. Chowdhury, E.M.A. Mokheimer. Recent developments in solar and low-temperature heat sources assisted power and cooling systems: A design perspective. ***J Energy Resour***, 142, 040801-1 - 040801-17, (2020).

[10] K. Comaklı. Economic and environmental comparison of the natural gas fired conventional and condensing combi-boilers. ***J. Energy Inst.***, 81, 242–246, (2008).

[11] A. Abusoglu, M. Kanoglu. Exergetic and thermodynamic analyses of diesel engine powered cogeneration. Part 1. Formulations. ***Appl. Therm. Eng.***, 29, 234–241, (2009).

[12] O.M. Ibrahim, S.A. Klein. Absorption power cycles. ***Energy***, 21, 21–27, (1996).

[13] D.S. Ayou, J.C. Bruno, R. Saravanan, A. Coronas. An overview of combined absorption power and cooling cycles**.** ***Renew Sustain Energy Rev***,, 21, 728–748, (2013).

[14] N. Shokati, F. Ranjbar, M. Yari. Exergoeconomic analysis and optimization of basic, dual-pressure and dual-fluid ORCs and Kalina geothermal power plants: A comparative study. ***Renewable Energy***, 83, 527-542, (2015).

[15] X.X. Zhang, M.G. He, Y. Zhang. A review of research on the kalina cycle**.** ***Renew Sustain Energy Rev***.,16, 5309–5318, (2012).

[16] A.I. Kalina. Combined cycle and waste-heat recovery power systems based on a novel thermodynamic energy cycle utilizing low-temperature heat for power generation. ***In 1983 Joint Power Generation Conference: GT Papers***, Indianapolis, IN, USA, 25–29 September, (1983).

[17] A.I. Kalina. Combined cycle system with novel bottoming cycle. ***J. Eng. Gas Turbines Power***, 106, 737–742, (1984).

[18] M. Jonsson. ***Advanced power cycles with mixtures as the working fluid.*** Diss. Royal Institute of Technology, Stockholm, Sweden, (2003).

[19] C.H. Marston. Parametric Analysis of the kalina cycle. ***J. Eng. Gas Turbines Power***, 112, 107–116, (1990).

[20] Y. Park, R. Sonntag. A preliminary study of the kalina power cycle in connection with a combined cycle system**.** ***Int. J. Energy Res.*****,** 14, 153–162, (1990).

[21] H.A. Mlcak. Kalina cycle concepts for low temperature geothermal. ***Geotherm Res Counc Trans*****,** 26, 707–713, (2002).

[22] C.E.C. Rodriguez, J.C.E. Palacio, O.J. Venturini, E.E.S. Lora, V.M. Cobas, D.M.D. Santos. Energetic and economic comparison of orc and kalina cycle for low temperature enhanced geothermal system in Brazil. ***Appl. Therm. Eng***., 52, 109–119, (2013).

[23] W. Fu, J. Zhu, T. Li, W. Zhang, J. Li. Comparison of a kalina cycle based cascade utilization system with an existing organic rankine cycle based geothermal power system in an oilfield. ***Appl. Therm. Eng***., 58, 224–233, (2013).

[24] M.H.D. Hettiarachchi, M. Golubovic, W.M. Worek, Y. Ikegami. The performance of the kalina cycle system 11(KCS-11) with low-temperature heat sources. ***J Energ Resour***, 129, 243–247, (2007).

[25] V. Zare, S.M.S. Mahmoudi. A thermodynamic comparison between organic rankine and kalina cycles for waste heat recovery from the gas turbine-modular helium reactor. ***Energy*****,** 79, 398–406, (2015).

[26] S. Li, Y. Dai. Thermo-economic comparison of kalina and CO_2 transcritical power cycle for low temperature geothermal sources in China. ***Appl. Therm. Eng*****.,** 70, 139–152, (2014).

[27] K. Chunnanond, S. Aphornratana. Ejectors: applications in refrigeration technology. ***Renew. Sustain. Energy Rev.*****.**, 8, 129–155, (2004).

[28] C. Seckin, Effect of ejector internal efficiencies on cooling performance of an ejector expansion refrigeration cycle with a two phase ejector. **In** ***International Conference on Energy and Thermal Engineering: ICTE 2017***, Istanbul, Turkey, 25–28 April, 152–161, (2017).

[29] C. Seckin, Thermodynamic analysis of a combined power/refrigeration cycle: combination of kalina cycle and ejector refrigeration cycle. ***Energy Convers. Manage***, 157, 631–643, (2018).

[30] C. Seckin. Parametric analysis and comparison of ejector expansion refrigeration cycles with constant area and constant pressure ejectors. ***J Energy Resour***,139, s042005-1–042005-10, (2017).

[31] Seckin, C. Effect of operational parameters on a novel combined cycle of ejector refrigeration cycle and kalina cycle. ***J Energy Resour***,142, 012001-1– 012001-11, (2020).

[32] L. Boumaraf, A. Lallemand. Modeling of an ejector refrigerating system operating in dimensioning and off-dimensioning conditions with the working fluids R142b and R600a. ***Appl Therm Eng*****,** 29, 265–274, (2009).

[33] Z. Aidoun, K. Ameur, M. Falsafioon, M. Badache. Current advances in ejector modeling, experimentation and applications for refrigeration and heat pumps. part 1: single-phase ejectors. ***Inventions,*** 4*,* 1-73, (2019).

[34] J. Wang, Y. Dai, T. Zhang, S. Ma. Parametric analysis for a new combined power and ejector absorption refrigeration cycle. ***Energy***, 34(10), 1587–1593, (2009).

[35] X.X. Xu, C. Liu, X. Fu, H. Gao, Y. Li. Energy and exergy analyses of a modified combined cooling, heating, and power system using supercritical CO_2. ***Energy*****,** 86, 414–422, (2015).

[36] J.F. Wang, P. Zhao, X. Niu, Y. Dai. Parametric analysis of a new combined cooling, heating, and power system with transcritical CO_2 driven by solar energy. ***Appl Energy***, 94, 58–64, (2012).

[37] A. Habibzadeh, M.M. Rashidi, N. Galanis. Analysis of a combined power and ejector refrigeration cycle using low temperature heat. ***Energy Convers Manage*****,** 65, 381–391, (2013).

[38] H. Ghaebi, H. Rostamzadeh, P.S. Matin. Performance evaluation of ejector expansion combined cooling and power cycles. ***Heat Mass Transf***, 4, 1–17, , (2017).

[39] O. Barkhordarian, A. Behbahaninia, R. Bahrampoury. A novel ammonia-water combined power and refrigeration cycle with two different cooling temperature levels. ***Energy***, 120, 816–826, (2017).

[40] W. Sun, X. Yue, Y. Wang. Exergy efficiency analysis of ORC (organic rankine cycle) and ORC-based combined cycles driven by low-

temperature waste heat. ***Energy Convers Manage***, 135, 63–73, (2017).

[41] H. Ghaebi, T. Parikhani, H. Rostamzadeh, B. Farhang. Thermodynamic and thermoeconomic analysis and optimization of a novel combined cooling and power (CCP) cycle by integrating of ejector refrigeration and kalina cycles. ***Energy***, 139, 262–276, (2017).

[42] G. Besagni, R. Mereu, F. Inzoli. Ejector refrigeration: a comprehensive review. ***Renew Sustain Energy Rev***, 53, 373–407, (2016).

[43] J.A.E. Carrillo, S. de La Flor, J.M. Salmeron Lissen. Thermodynamic comparison of ejector cooling cycles. ejector characterization by means of entrainment ratio and compression efficiency. ***Int. J. Refrig.***, 74, 371–384, (2017).

[44] M. Sokolov, D. Hershgal. Enhanced ejector refrigeration cycles powered by low grade heat. Part 1. Systems characterization. ***Int. J. Refrig.***, 13, 351-356, (1990).

[45] E. Thorin. ***Power cycles with ammonia-water mixtures as working fluid - analysis of different applications and the influence of thermophysical properties***. Diss. Royal Institute of Technology, Stockholm, Sweden, (2000).

[46] S. Ogriseck. Integration of kalina cycle in a combined heat and power plant, a case study. ***Appl. Therm. Eng***., 29, 2843–2848, (2009).

[47] R. Yapıcı, H.K. Ersoy. Performance characteristics of the ejector refrigeration system based on the constant area ejector flow model. ***Energy Convers. Manage.***, 46, 3117–3135, (2005).

[48] H.K. Ersoy, S. Yalcin, R. Yapici, M. Ozgoren Performance of a solar ejector cooling-system in the southern region of Turkey. ***Appl. Energy***, 84, 971–983, (2007).

[49] A. Khalil, M. Fatouh, E. Elgendy. Ejector design and theoretical study of R134a ejector refrigeration cycle. ***Int. J. Refrig.***, 34(7), 1684–1698, (2011).

[50] L. Cao, J. Wang, Y. Dai. Thermodynamic analysis of a biomass-fired kalina cycle with regenerative heater. *Energy*, 77, 760–770, (2014).

[51] M. Ahmad, M.N. Karimi. Thermodynamic analysis of kalina cycle. ***Int. J. Sci. Res.***, 5, 2244–2249, (2016).

[52] G.K. Alexis, E.K. Karayiannis. A solar ejector cooling system using refrigerant R134a in the Athens area. ***Renewable Energy***, 30, 1457–1469, (2005).

[53] R.E. Henry, H.K. Fauske. The two-phase critical flow of one component mixtures in nozzles, orifices, and short tubes. ***J Heat Transf***, 93, 179–187, (1971).

[54] C. Seckin. Investigation of the effect of the primary nozzle throat diameter on the evaporator performance of an ejector expansion refrigeration cycle. ***J. Therm. Eng.***, 4, 1939-1953, (2018).

[55] M. Hassanain, E. Elgendy, M. Fatouh. Ejector expansion refrigeration system: ejector design and performance evaluation. ***Int J Refrig.***, 58, 1–13, (2015).

[56] F.H. Shu, *The physics of astrophysics. Vol.2: Gas dynamics*. ***University Science Books***, Mill Valley, (1991).

[57] J. Szargut, D.R. Morris, F.R. Steward. Exergy analysis of thermal, chemical, and metallurgical processes. ***Hemisphere Publishing Corporation***, NY, USA, (1988).

[58] M. Atmaca, C. Ezgi. Three-dimensional CFD modeling of a steam ejector. ***Energy Sources A: Recovery Util. Environ. Eff***., 44, 2236-2247, (2022).

[59] M. Gumus, M. Atmaca. Energy and exergy analyses applied to a CI engine fueled with diesel and natural gas. ***Energy Sources A: Recovery Util. Environ. Eff.***, 35, 1017–1027, (2013).